Characterization and Photocatalytic Activity of ZnO, ZnS, ZnO/ZnS, CdO, CdS and CdO/CdS Nanoparticles in Mesoporous SBA-15

Pouretedal, Hamid Reza*[+]

Faculty of Applied Chemistry, Malek-ashtar University of Technology, Shahin-Shahr, I.R. IRAN

Basati, Sara

Department of Chemistry, Islamic Azad University, Shahreza Branch, Shahreza, I.R. IRAN

ABSTRACT: *Grinding (solvent-free) method was used as a superior technique to prepare mesoporous photocatalysts of ZnO, ZnS, ZnO / ZnS, CdO, CdS and CdO / CdS-SBA-15. In this technique, the nitrate, acetate and chloride salts of zinc and/or cadmium were grinded with as-synthesized SBA-15 as a mesoporous material. The controllable sulfurationis was used to prepare ZnS, ZnO/ZnS, CdS and CdO/CdS-SBA-15 at temperature of 80 °C. The advantages of grinding technique were: i) the elimination of solvent and thus decrease of expense and ii) the complete incorporation of metal salts in the nanochannel of mesoporous material in a short time. X-ray powder diffraction, N_2 adsorption-desorption and FT-IR spectroscopy were used to characterize the prepared materials. The highly dispersed semiconductors in SBA-15 demonstrate an active photodegradation of Congo red in aqueous solution. The nanocomposites of ZnO/ZnS and CdO/CdS in channels of SBA-15 showed the highest photocatalytic activity. The photocatalytic activity of ZnO-, ZnS- and ZnO/ZnS-SBA-15 were also dependent on the salt precursor of zinc. The prepared composite photocatalysts of zinc/SBA-15, by using $ZnCl_2$ as salt precursor, indicated the higher activity.*

KEY WORDS: *Photocatalyst, SBA-15, Nanoparticles, Congo red, zinc, Cadmium.*

INTRODUCTION

The Ordered Mesoporous Materials (OMMs) with the porous nature and high surface area are used as substrate for catalysts [1,2]. The SBA-15 is a type of ordered mesoporous materials that can act as a molecular sieve. Due to formation of SBA-15 with a symmetry of two-dimensional P6mm [3], the triblock copolymer surfactants are suitable templates. The arrays of SBA-15 are hexagonal with pore diameters in the range of 5–30 nm. High surface area, narrow pore size distribution and high pore volume are several important advantages of SBA-15 [4,5]. However, the SBA-15 shows a high potential for incorporation of metals, metal oxides and metal sulfides [6,7]. Increasing of catalytic reactivity of metal oxides and metal sulfides in mesoporous material of SBA-15

* *To whom correspondence should be addressed.*
+ E-mail: hr_ pouretedal@mut-es.ac.ir
1021-9986/15/1/11 9/$/2.90

is expected because the prepared catalyst has large surface area.

For synthesis process of mesoporous materials, the size growth of catalyst nanoparticles and their shape as well as their appearance and stabilization are controllable [8]. The catalyst nanotubes can be formed as a narrow layer in the inner walls of the mesoporous silica. Also, the formation of nanocomposite catalysts by using the various semiconductors such as metal oxides and metal sulfides is a merit of mesoporous materials [9]. The creation of nanocomposite catalysts can increase photocatalytic activity. The existence of nanochannels (5-10 nm) and the stability of thermal and hydrothermal of SBA-15 provide this mesoporous silica material as an important candidate for using as substrate of photocatalysts [10].

The creation of a nanocomposite is one of the ways for increasing the photocatalytic activity of photocatalysts. As usual, the nanocomposites show high quality properties with respect to their pure components. The nanocomposite CdS/CdSe with structure of core-shell can produce intensephotoluminescence with high quantum yield [11]. The increase of photoluminescence intensity of CdS/CdSe nanocomposite arises from passivation of CdSe nanoparticles surface by nanosized ZnS [12]. Shen and co-workers show the photocatalytic reactivity of nanosized TiO_2, which can be increased by formation of TiO_2–CdSe nanocomposite [13]. The coupling of ZnO nanopowder with CdS and CdSe can increase appreciably the Incident Photons Current Conversion Efficiency (IPCE%) of zinc oxide nanoparticles [14]. The zinc oxide semiconductor acts as a photocatalyst in UV region of radiation [15]. However, synthesis of ZnO-CdS and ZnO-CdSe nanocomposite, by a simple and cheap method, gives the zinc oxide nanoparticles activein visible region [16]. For a synthesized nanocomposite, the individual components can show suitable advantages. For example, in CdS–ZnO nanocomposite, cadmium sulfide with band-gap energy (Eg) of 2.4 eV acts as a visible sensitizer. While, zinc oxide (Eg = 3.34 eV) can help to separate holes and electrons as well as decreasing rate and probability of charge recombination in semiconductor [17]. The formation of nanocomposites as nanorods has a preference versus nanoparticles because they indicate a smaller volume density of point defects in composite structures.

The purpose of this work is to synthesize mesoporous photocatalysts of ZnO, ZnS ZnO/ZnS, CdO, CdS and CdO/CdS-SBA-15 by using a solvent-free (grinding) method. The characterization of prepared materials are performed and the photocatalytic activity are also studied in this research.

EXPERIMENTAL SECTION

Synthesis of photocatalysts

The SBA-15 was prepared by a process modified from Ref. [18-20]: 2 g of triblock copolymer P123 ($EO_{20}PO_{70}EO_{20}$, average molecular weight = 5,800, Aldrich) was dissolved in a solution of 60 g 2 M HCl and 15 g H_2O at room temperature at first, then followed by the addition of 4.5 g of TEOS (tetraethylorthosilicate, Aldrich Co.). The mixture was stirred at 40 ^oC for 24 h, then transferred into an autoclave for further condensation at 100 ^oC for 2 days. The final solid was collected by filtration, washed with distilled water,and dried at room temperature. The surfactants were removedby calcinations at 550 ^oC for 6 h.

The ZnS-, ZnO-, ZnO/ZnS-, CdS-, CdO- and CdO/CdS-SBA-15 photocatalysts were synthesized by procedure mentioned for SBA15. After preparation of SBA15 and before calcinations step, the SBA-15 was manually ground with the calculated amount ofzinc nitrate and/or cadmium nitrateat room temperature so that the content of zinc and/or cadmium was 40% in prepared photocatalysts. In general, the resulting homogeneous powder of $Zn(NO_3)_2$- and $Cd(NO_3)_2$-SBA15 was calcined at 550 ^oC with rate of 2 ^oC/min for 5 h in air with a flow of 100mL/min. Then, ZnO-SBA-15 and CdO-SBA15 powders were obtained. In order to obtain the ZnS-SBA-15 and ZnO/ZnS-SBA15, the requisite amount of thioacetamide (TAA) was added to ZnO-SBA-15 powder and the mixture was heated in an autoclave at 80 ^oC for 6 h. The ratio of ZnS and ZnO in the prepared composite (ZnO/ZnS-SBA15) was 1:1. The CdS-SBA15 and CdO/CdS-SBA15 photocatalysts were synthesized by the same procedure with the CdO-SBA15 powder as precursor. The chloride and acetate salts were used to study the effect of salt anion on the modification of substrate and photocatalytic activity of ZnO/ZnS-SBA-15.

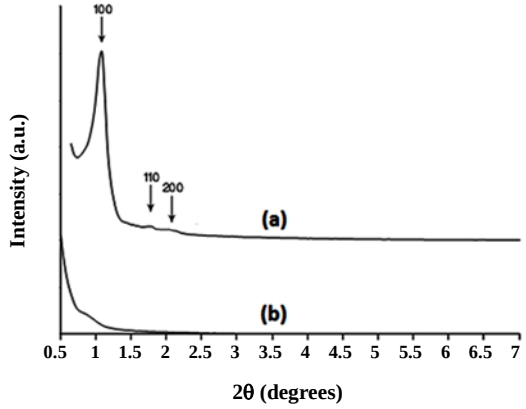

Fig. 1: XRD patterns of (a) Si-SBA-15 and (b) ZnO/ZnS-SBA-15 at low-angle with content of 40% zinc.

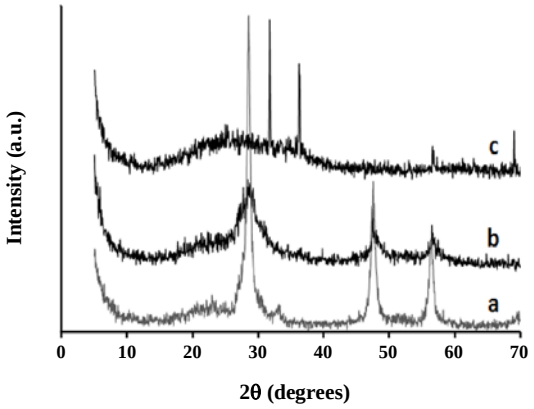

Fig. 2: XRD pattern of (a) ZnS/SBA-15, (b) ZnO/ZnS-SBA-15 and (c) ZnO/SBA-15 at wide-angle with content of 40% zinc.

Characterization of nanoparticles

Nicolet Impact 400D FT-IR Spectrophotometer was used to record the IR-spectra of prepared photocatalysts (pressed discs with KBr) in range 4000-400 cm^{-1}. A Diffractometer Bruker D8ADVANCE Germany with anode of Cu (λ=1.5406 Å of Cu K_α) and filter of Ni applied to record of X-ray diffraction (XRD) patterns of nanoparticles and mesoporous SBA-15 in the 2θ ranges from 0.5 to 7° or from 5 to 70°. The surface of prepared photocatalysts were estimated by the B.E.T. method and N_2 adsorption isotherms. The nitrogen as an adsorption gas at 77 K using a Belsorp Mini Π instrument was used in this study. Samples were out gassed at 300 °C for 4 h prior to surface area measurements. The EDX spectra of prepared ZnO/ZnS and CdO/CdS nanocomposites were obtained by a Philips XL 30 Scanning Electron Microscope (SEM).

Activity of the photocatalysts

The activity of prepared photocatalysts was studied in photodegradation of Congo red (CR) as a dye pollutant. A photocatalytic reactor with a 36 W mercury low pressure lamp as irradiation source was used to perform of photodegradation reactions. The light path was 3.0 cm in photoreactor cell. The photoreactor filled with 20 mL of 10-50 mg/L of CR and 0.1-1.0 g/L of ZnS-, ZnO-, ZnO/ZnS-, CdS-, CdO- and CdO/CdS-SBA-15 photocatalysts. The whole reactor cooled with a water-cooled jacket on its outside and the temperature was kept at 25 °C. All reactants in a degradation reaction were stirred using a magnetic stirrer to uniform of photoreactor cell. In order to setting the adsorption/desorption equilibrium of CR on heterogeneous catalysts surface, the reactor was kept in dark conditions within 30 min.

Thedegradation efficiency of CR determined with measurement of absorbance of samples by a UV-Vis spectrophotometer Carry-100 using a paired 1.0 cm quartz cell. The samples centrifuged to remove the heterogeneous photocalatlysts before absorbance measurement. The absorbance of samples before (A_o) and after a distinct time (A_t) of irradiation and Beers' law were used for calculate of degradation efficiency (Eq. (1)). The dosage of photocatalysts were also investigated on the degradation efficiencies.

$$\%\text{Degradation} = 100 \times [1- (C_t/C_o)] = 100 \times [1-(A_t/A_o)] \quad (1)$$

RESULTS AND DISCUSSION

Characterization of photocatalysts

The X-ray diffraction patterns of SBA-15 and ZnO/ZnS-SBA-15 at low-angle and ZnO-, ZnS-, ZnO/ZnS-SBA-15 at wide-angle are indicated in Figs. 1 and 2, respectively. The prepared samples are calcined at 550 °C. The XRD pattern (Fig. 1a) with a projecting peak (100) at 2θ = 1.09° and two weak peaks (110) and (200) at 2θ = 1.73 and 1.97° show a p6mm hexagonal lattice symmetry for SBA-15 [18,20]. The XRD pattern of ZnO/ZnS-SBA-15 (Fig. 1b) and the decrease the intensity of projecting the peak (100) indicates complete dispersion of zinc oxide and zinc sulfide in channels of SBA-15. In other words, in nanocomposite of ZnO/ZnS-SBA-15, Si cations are substituted by zinc cations in grinding and heating steps of prepared sample. The intense decrease of

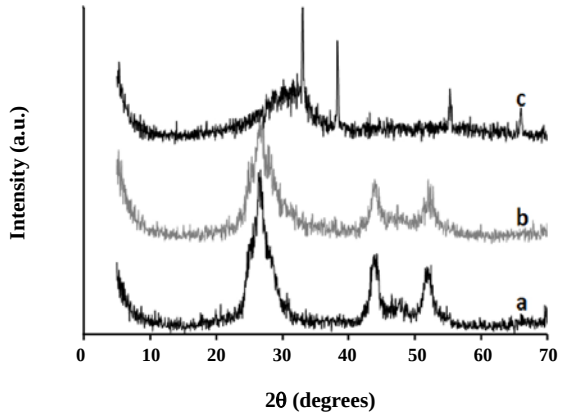

Fig. 3: XRD pattern of (a) CdS/SBA-15, (b) CdO/CdS-SBA-15 and (c) CdO/SBA-15 at wide-angle with content of 40% cadmium.

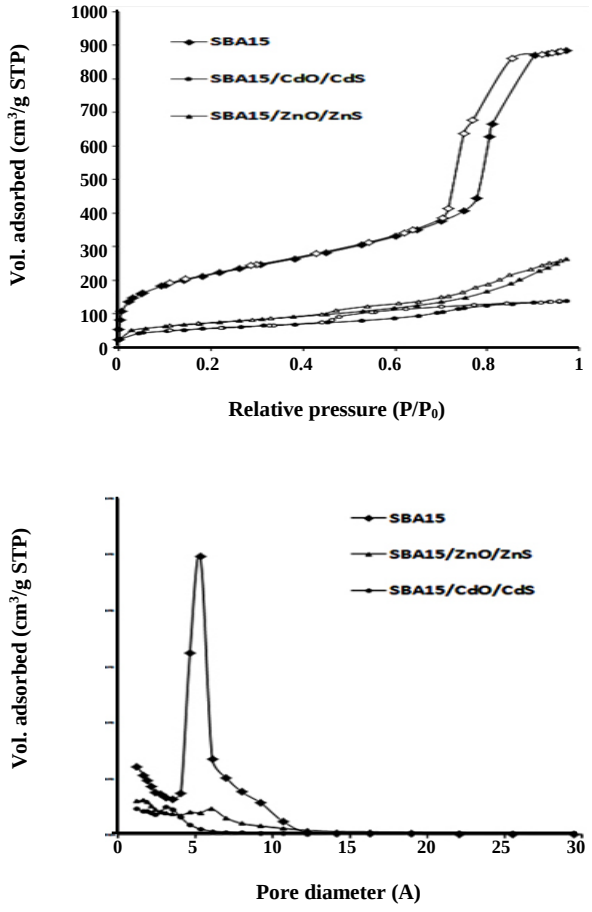

Fig. 4. (a) Nitrogen adsorption–desorption isotherms and (b) pore distribution curves of calcined SBA-15, ZnO/ZnS-SBA-15 and CdO/CdS-SBA-15.

characteristic peaks of SBA-15 can be due to powerful interaction ZnO/ZnS with substrate. The nugatory variation of peak location (100) in XRD pattern of ZnO/ZnS-SBA-15 and SBA-15 indicates protection of SBA-15 structure with mesoscopic order [20]. In Fig. 2, a broad peak at 2θ approximately 23° is seen that shows an amorphous structure of SBA-15 wall [1-4].

Zinc oxide crystallizes in two main forms, hexagonal wurtzite and cubic zincblende [21,22]. The wurtzite structure is most stable at ambient conditions and thus most common. The hexagonal wurtzite of ZnO nanoparticles is confirmed with prominent peaks of (100), (101) and (110) at 2θ = 32.2, 37.1 and 57.3° (Fig. 2c). Also, as seen from Fig. 2a and 2b, the diffraction peaks at 2θ = 28.5°, 47.6°, 56.5° correspond to (111), (220) and (311) planes show the formation of cubic cell of ZnS nanoparticles (zinc blende structure with JCPDS card, File No. 79–0043) with unit cell parameter a_o = 3.61 Å. Thus, it is observed that ZnO is converted to ZnS in TAA aqueous solution at 40 °C. TAA can be rapidly released sulfide ion at elevated temperature under hydrothermal process. The Scherrer formula show the average crystal size of 15 nm for the ZnO and ZnS nanoparticles in substrate of SBA-15 [23,24].

The XRD patterns of CdO-, CdS-, CdO/CdS-SBA-15 at wide-angle are also shown in Fig. 3. As seen, the intensity of broad peak at 2θ = 23° is decreased that show the destruction of amorphous structure of SBA-15 walls. The larger ionic size of Cd^{2+} ions versus Zn^{2+} ions can be due to damaging of SBA-15 walls. The peak at about 27° and peaks of 30.9, 44.2 and 52.4° in CdS/SBA-15 and 30.4, 43.9, 47.3 and 51.9° at CdO/CdS-SBA-15, show the formation of cubic cell of CdS which are very close to the values in the literature [25,26]. As well as of ZnO/SBA-15, the hexagonal wurtzite structure of CdO nanoparticles on the substrate of SBA-15 is seen in Fig. 3c. The broadening of the peaks in XRD patternindicates the formation of CdS nanoparticles with average size of 6 nm (Scherrer formula) that adapted pore diameter of themodified SBA-15.

The nitrogen adsorption–desorption isotherms and pore volume distribution of SBA-15, ZnO/ZnS-SBA-15 and CdO/CdS-SBA-15 are shown in Fig. 4. The type of IV-isotherm is seen from these isotherms for prepared mesoporous materials according to IUPAC definitions [27]. Avigorous adsorption in arelative pressure range of

Table 1: The N_2 adsorption–desorption of SBA-15, ZnO/ZnS-SBA-15 and CdO/CdS-SBA-15 composites.

Photocatalyst	BET data			BJH data		
	S_{BET} (m^2/g)	V_p (cm^3/g)	D_p (nm)	S_{BET} (m^2/g)	V_p (cm^3/g)	D_p (nm)
SBA-15	781.48	1.36	6.99	697.65	1.29	4.03
ZnO/ZnS-SBA-15	257.90	0.40	6.28	241.76	0.38	1.85
CdO/CdS-SBA-15	194.35	0.21	4.39	181.87	0.19	1.80

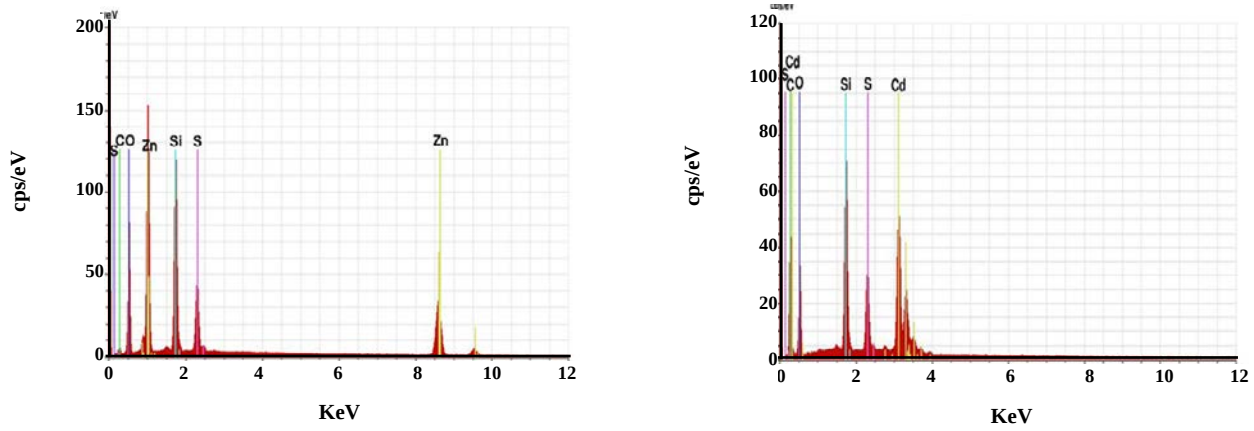

Fig. 5: EDX spectrum of (a) ZnO/ZnS-SBA-15 and (b) CdO/CdS-SBA-15.

$\sim 0.7 < P/P_o < 0.9$ is observed for prepared SBA-15 that is a marked of capillary uniform arrays of mesoporous materials. The suitable mesoporous structure and restricted distribution of pores size are indicated from adsorption–desorption isotherms. The specific surface area (S_{BET}), average pore diameter (D_p) and pore volume (V_p) calculated according to the standard BET and BJH methods [28,29] are collected in Table 1.

It is the decrease of pore volume of prepared catalysts that expected with deposition of zinc and cadmium ions in micropores of SBA-15 walls. The difference of mesopores diameter of Zn-SBA-15 and Cd-SBA-15 from SBA-15 is due to difference of ionic radii of Zn^{2+} (0.74 Å), Cd^{2+} (0.97 Å) and Si^{4+} (0.39 Å) and bond length of Zn–O and Cd–O from Si–O [22]. However, the reduction of pore volume indicates the considerable incorporation of zinc and cadmium ions into silicate framework and the formation of dispersed metal oxide and/or metal sulfide on the surface of SBA-15 [21,22].

The formation of ZnO/ZnS and CdO/CdS are also confirmed by using EDX analysis (Fig. 5). EDX spectra resulted from five dissimilarity selected regions. The average amount of 40 wt% of zinc and/or cadmium is approximately resulted from EDX spectra. The intensity of zinc and cadmium signals reveals that the ZnO/ZnS and/or CdO/CdS exist inside the channels of SBA-15.

Host–guest strong interaction plays a serious role in the high dispersion of ZnO/ZnS and/or CdO/CdS in SBA-15. The FT-IR absorption spectra of CdO/SBA-15 and ZnO/SBA-15 synthesized by grinding method and pure SBA-15 are shown in Figs. 6 and 7, respectively. As mentioned in the reports, the samples show a marked absorption band at ~3432 cm^{-1} that is related to the vibration absorption of silanol groups (Si–O–H) situated inside the channels of SBA-15 [4,5]. Three peaks at wave numbers of ~465, ~800, and ~1085 cm^{-1} are attributed to the rocking, bending (or symmetric stretching), and asymmetric stretching, respectively, of the inter-tetrahedral oxygen atoms in SiO_2 of SBA-15 [4]. Also, the absorption band at ~1085 cm^{-1} show the asymmetry vibration of Si–O–Si. The absorption band at ~950 cm^{-1} in the spectra of pure SBA-15 is related to the stretching vibrations of Si-O in the Si–O–R^+ groups [20-22].

The FT-IR spectra of CdO/SBA-15 and ZnO/SBA-15 indicate a shift in absorption peaks toward the lower wave number in comparison with SBA-15. This shift is

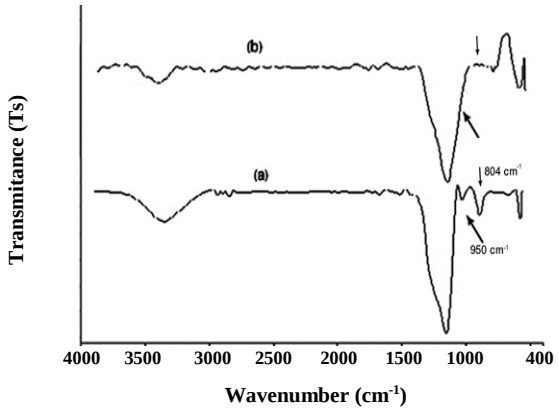

Fig. 6: FT-IR spectra of (a) CdO/SBA-15 and (b) SBA-15.

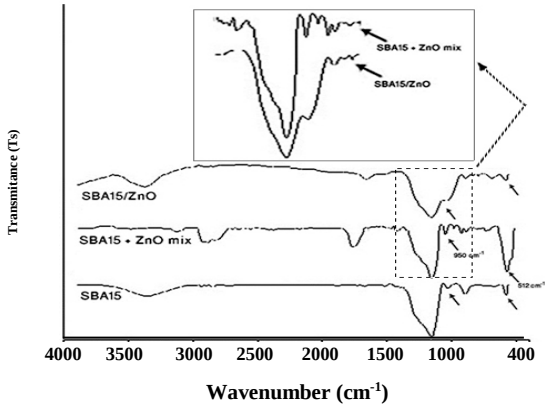

Fig. 7: FT-IR spectra of SBA-15, ZnO/SBA-15 and ZnO alone with the mixture of SBA-15 with 40 wt% ZnO.

a verification for incorporation of ZnO and/or CdO into the framework of SBA-15. The IR spectra of a mixture of SBA-15 and ZnO (with weight ratio of 60:40) are studied to investigate the host–guest interaction in the ZnO/SBA-15 sample (Fig. 7). Zinc oxide exhibits absorption band in the 600–400 cm^{-1} region with marked two peaks centered at 512 and 496 cm^{-1}, while the peaks around 960, 800 and 465 cm^{-1} are assigned to SBA-15. Mechanical mixing of SBA-15 with ZnO does not show the omission of marked absorption bandsof SBA-15 especially band centered 960 cm^{-1} (Fig. 7). However, the spectra of ZnO/SBA-15 catalyst and shift of band centered 960 cm^{-1} indicate the host–guest interaction of ZnO and SBA [20-22].

Photocatalytic activity

The kinetic rate constants of CR photodegradation process catalyzed by prepared photocatalysts are collected in Table 2. The pseudo-first-order rate constants, k_{obs} (min^{-1}), are obtained using Langmuir–Hinshelwood kinetic expression ($\ln (C_o/C_t) = k_{obs}t$) [26]. The photodegradation conditions are: CR; 10 mg/L, photocatalyst; 0.1 g/L and pH; 7. The photodegradation of CR is also compared at presence of SBA-15 in dark and under irradiation. The reduction of CR concentration in dark and at presence of SBA-15 is related to surface adsorption of mesoporous materials. However, under irradiation, SBA-15 did not show any photocatalytic activity.

As seen from Table 2 data, the presence of ZnS, ZnO, CdS and CdO on the substrate of SBA-15 due to an increasing in photocatalytic activity. Increasing the surface area of photocatalyst with incorporation of zinc and/or cadmium in mesopours substrate in comparisonto ZnS, ZnO, CdS and CdO alone is a contented reason for increasing of photocatalytic activity. The semiconductors of CdS (2.5 eV) and CdO (2.3 eV) with the less band-gap energies due to higher photocatalytic activity versus ZnO (3.3 eV) and ZnS (3.7 eV). However, the nanocomposite of ZnO/ZnS-SBA-15 and CdO/CdS-SBA-15 shows the highest photocatalytic activity. The formation of solid solution between ZnS and ZnO or CdS and CdO seemed due to a red-shift and thus decreasing of band-gap energy [30,31].

The data of Table 3 indicates the influence of salt precursor of zinc such as chloride, nitrate and acetate on the pseudo-first-order rate constants of photodegradation reaction. The highest photocatalytic activity is obtained with chloride anion of zinc salt in preparation process of ZnO-, ZnS- and ZnO/ZnS-SBA-15 in grinding method. Apparently, the incorporation of zinc ions in SBA-15 channels is more effective with using $ZnCl_2$ as precursor. Therefore, it is expected the increase of weight percent of ZnS and/or ZnO in prepared composite.

The effect of photocatalyst dose (0.1-1.0 g/L) and initial concentration of CR (10-50 mg/L) is also studied on the photodegradation efficiency at presence of ZnO/ZnS-SBA-15 as photocatalyst. The obtained results demonstrate that the 0.7 g/L of ZnO/ZnS-SBA-15 is an optimum dose for photocatalyst. Also, the degradation efficiency of CR is decreased with increasing of initial concentration of dye. So that, the degradation efficiency of CR decrease from 92.6 to 62.3% with increasing of CR concentration from 10 to 50 mg/L.

Table 2: The pseudo-first-order rate constants of CR photodegradation reaction catalyzed by prepared photocatalysts. The nitrate salt of zinc and cadmium is used as precursor.

Photocatalyst	k_{obs} (min^{-1})	Photocatalyst	k_{obs} (min^{-1})	Photocatalyst	k_{obs} (min^{-1})
-	6.4×10^{-3}	ZnS	14.9×10^{-3}	CdS-SBA-15, NO_3	19.9×10^{-3}
SBA-15, Dark	0.5×10^{-3}	CdS	15.7×10^{-3}	ZnO/ZnS-SBA-15, NO_3	23.9×10^{-3}
SBA-15	6.6×10^{-3}	ZnO-SBA-15, NO_3	20.6×10^{-3}	CdO/CdS-SBA-15, NO_3	28.3×10^{-3}
ZnO	10.1×10^{-3}	CdO-SBA-15, NO_3	22.0×10^{-3}		
CdO	11.0×10^{-3}	ZnS-SBA-15, NO_3	19.1×10^{-3}		

Table 3: Influence of the salt precursor of zinc on the pseudo-first-order rate constants of CR photodegradation reaction catalyzed by prepared photocatalysts of Zn-SBA-15.

Photocatalyst	k_{obs} (min^{-1})	Photocatalyst	k_{obs} (min^{-1})
ZnO-SBA-15, Cl	23.1×10^{-3}	ZnS-SBA-15, OAC	21.6×10^{-3}
ZnO-SBA-15, NO_3	20.6×10^{-3}	ZnO/ZnS-SBA-15, Cl	30.4×10^{-3}
ZnO-SBA-15, OAC	22.8×10^{-3}	ZnO/ZnS-SBA-15, NO_3	23.9×10^{-3}
ZnS-SBA-15, Cl	25.7×10^{-3}	ZnO/ZnS-SBA-15, OAC	25.6×10^{-3}
ZnS-SBA-15, NO_3	19.1×10^{-3}		

The turbidity of the suspension of heterogeneous photocatalyst at high dose is due to decrease of radiation penetration in photoactivated volume of suspension and thus of penetration depth of the photons. The high adsorption of CR molecules on the substrate, decreasing generation of hydroxyl radicals in active sites and increasing absorption of photons by dye molecules are due to reduction of degradation efficiency at high concentrations of dye [32].

CONCLUSIONS

The grinding method can be used for preparation of metal oxide and/or metal sulfide incorporated mesoporous material of SBA-15. The photocatalytic activity of ZnO, ZnS, CdO and CdS in substrate of SBA-15 are increasedbecause the increasing of surface area of prepared photocatalyst. The selection of salt precursor of zinc can be influencedin the incorporation of zinc ions in pores of SBA-15. The chloride salt is a superior salt in grinding procedure.

Received : Dec. 29, 2013 ; Accepted : Sep. 26, 2014

REFERENCES

[1] Kresge C.T., Leonowicz M.E., Roth W.J., Vartuli J.C., Beck J.S., Ordered Mesoporous Molecular Sieves Synthesized by a Liquid-Crystal Template Mechanism, *Nature* **359**: 710-712 (1992).

[2] Zhang W.H., Shi J.L., Chen H.R., Hua Z.L., Yan D.S., Synthesis and Characterization of Nanosized ZnS Confined in Ordered Mesoporous Ssilica, *Chem. Mater.* **13**: 648-654 (2001).

[3] Zhao D., Feng J., Huo Q., Melosh N., Fredrickson G.H., Chmelka B.F., Stucky G.D., Triblock Copolymer Syntheses of Mesoporous Silica with Periodic 50 to 300 Angstrom Pores, *Science*, **279**: 548-552 (1998).

[4] Ziarani G.M., Mousavi S., Lashgari N., Badiei A., Shakiba M., Application of Sulfonic Acid Functionalized Nanoporous Silica (SBA-Pr-SO_3H) in the Green One-Ppot Synthesis of Polyhydroacridine Libraries, *Iran. J. Chem. Chem. Eng. (IJCCE)*, **32**: 9-16 (2013).

[5] Zhao D., Huo Q., Feng J., Chmelka B.F., Stucky G.D., Stucky, Nonionic Triblock and Star Diblock Copolymer and Oligomeric Surfactant Syntheses of Highly Ordered, Hydrothermally Stable, Mesoporous Silica Sructures, *J. Am. Chem. Soc.* **120**: 6024-6036 (1998).

[6] Segura Y., Cool P., Van Der Voort P., Mees F., Meynen V., Vansant E.F., TiO_x-VO_x Mixed Oxides on SBA-15 Support Prepared by the Designed Dispersion of Acetylacetonate Complexes: Spectroscopic Study of the Reaction Mechanisms, *J. Phys. Chem. B*, **108**: 3794-3800(2004).

[7] Busuioc, A.M., Meynen, V., Beyers, E., Mertens, M., Cool, P., Bilba, N., Vansant, E.F., Structural Features and Photocatalytic Behaviour of Titania Deposited within the Pores of SBA-15, *Appl. Catal. A* **312**: 153-164 (2006).

[8] Perathoner, S., Lanzafame, P., Passalacqua, R., Centi, G., Schlogl, R., Su, D.S., Use of Mesoporous SBA-15 for Nanostructuringtitania for Photocatalytic applications, *Micropor. Mesopor. Mater.* **90**: 347-361 (2006).

[9] Ciesla, U., Schuth, F., Ordered Mesoporous Materials, *Micropor. Mesopor. Mater.* **27**: 131-149 (1999).

[10] Lopez-Munoz M.J., van Grieken R., Aguado J., Marugan, J., Role of the Support on the Activity of Silica-Supported TiO_2 Photocatalysts: Structure of the TiO_2/SBA-15 Photocatalysts, *Catal. Today*, **101**: 307-314 (2005).

[11] Peng X., Schlamp M.C., Kadavanchi A.V., Alivisatos A.P., Epitaxial Growth of Highly Luminescent CdSe/CdS Core/Shell Nanocrystals with Photostability and Electronic Accessibility, *J. Am. Chem. Soc.* **119**: 7019-7029(1997).

[12] Dabbousi B.O., Jensen K.F., Bawendi M.G., (CdSe) ZnS Core-Shell Quantum Dots: Synthesis and Characterization of a Size Series of Highly Luminescent Nanocrystallites, *J. Phys. Chem. B* **101**: 9463-9475(1998).

[13] Janitabar D.S., Mahjoub A.R., Nilchi A., Synthesis of Spongelike Mesoporous Anatase and Its Photocatalytic Properties, *Iran. J. Chem. Chem. Eng. (IJCCE)*, **29**: 37-42 (2010).

[14] Hotchandani S., Kamat P.V., Charge-Transfer Processes in Coupled Semiconductor Ssystems. Photochemistry and Photoelectrochemistry of the Colloidal Cadmium Sulfide-zinc Oxide Ssystem, *J. Phys. Chem.* **96**: 6834-6839 (1992).

[15] Modirshahla N., Behnajady M.A., Jangi Oskui M.R., Investigation of the Eefficiency of ZnO Photocatalyst in the Removal of p-Nitrophenol from Contaminated Water, *Iran. J. Chem. Chem. Eng. (IJCCE)*, **28**: 49-55 (2009).

[16] Vayssieres L., Kies K., Lindquist S.E., Hagfeldt A., Purpose-Built Anisotropic Metal Oxide Material: 3D Highly Oriented Microrod Array of ZnO, *J. Phys. Chem. B* **105**: 3350-3352 (2001).

[17] Nayak J., Sahu S.N., Kasuya J., Nozaki S., CdS-ZnO Composite Nanorods: Synthesis, Characterization and Application for Photocatalytic Degradation of 3,4-dDihydroxy Benzoic Acid, *Appl. Sur. Sci.* **254**: 7215-7218 (2008).

[18] Yang H.C., Lin C.Y., Chien Y.S., Wu J.C.S., Wu H.H., Mesoporous TiO_2/SBA-15, and Cu/TiO_2/SBA-15 Composite Photocatalysts for Photoreduction of CO_2 to Methanol, *Catal. Lett.* **131**: 381-387 (2009).

[19] Xia F., Ou E., Wang L., Wang J., Photocatalytic Degradation of Dyes Over Cobalt Doped Mesoporous SBA-15 Under Sunlight, *Dyes Pigments* **76**:. 76-81 (2008).

[20] Lunawat P.S., Kumar R., Gupta N.M., Structure Sensitivity of Nano-Structured CdS/SBA-15 Containing Au and Pt Co-Catalysts for the Photocatalytic Splitting of Water, *Catal. Lett.* **121**: 226-233 (2008).

[21] Jiang Q., Wu Z.Y., Wang Y.M., Cao Y., Zhou C.F., Zhu J.H., Fabrication of Photoluminescent ZnO/SBA-15 Through Directly Dspersing Zinc Nitrate Into the As-Pprepared Mesoporous Silica Occluded with Template, *J. Mater. Chem.*, **16**: 1536-1542(2006).

[22] Gu F.N., Yue M.B., Wu Z.Y., Sun L.B., Wang Y., Zhu J.H., Enhanced Blue Emission from ZnS–ZnO Composites Confined in SBA-15, *J. Luminescence* **128**: 1148-1154 (2008).

[23] Pouretedal H.R., Keshavarz M.H., Synthesis and Characterization of $Zn_{1-X}Cu_XS$ and $Zn_{1-X}Ni_XS$ Nanoparticles and Their Applications as Photocatalyst in Congo Red Degradation, *J. Alloys Comp.*, **501**: 130-135(2010).

[24] Pouretedal H.R., Narimany S., Keshavarz M.H., Nanoparticles of ZnS Doped with Iron as Photocatalyst Under UV and Sunlight Irradiation, *Int. J. Mat. Res.*, **101**: 1046-1051 (2010).

[25] Zu S., Wang Z., Liu B., Fan X., Qian G., Synthesis of Nano-$Cd_xZn_{1-x}S$ by Precipitate-Hydrothermal Method and Its Photocatalytic Activities, *J. Alloys Comp.*, **476**: 689-692 (2009).

[26] Pouretedal H.R., Eskandari H., Keshavarz M.H., Semnani A., Photodegradation of Organic Dyes Uing Nanoparticles of Cadmium Sulfide Doped with Manganese, Nckel and Copper as Nanophotocatalyst, *Acta Chim. Slov.*, **56**: 353- 361(2009).

[27] Gregg S.J., Sing K.S.W., "Adsorption, Surface Area and Porosity", 2nd ed., Academic Press, London, 1982.

[28] Brunauer S., Emmett P.H., Teller E., Adsorption of Gases in Multimolecular Layers, *J. Am. Chem. Soc.*, **60**: 309-319 (1938).

[29] Kruk, M., Antchshuk, V., Jaroniec, M., Sayari, A., New Approach to Evaluate Pore Size Distributions and Surface Areas for Hydrophobic Mesoporous Solids, *J. Phys. Chem. B* 103, p. 10670-10678 (1999).

[30] Movahedi M., Mahjoub A.R., Janitabar-Darzi S., Photodegradation of Congo Red in Aqueous Solution on ZnO as an Alternative Catalyst to TiO_2, *J. Iran. Chem. Soc.*, **6**: 570-577(2009).

[31] Jang J., Yu C.J., Choi S.H., Ji S.M., Kim E.S., Lee J.S., Topotactic Synthesis of Mesoporous ZnS and ZnO Nanoplates and Their Photocatalytic Activity, *J. Catal.*, **254**: 144-155 (2008).

[32] Pouretedal H.R., Keshavarz M.H., Yosefi M.H., Shokrollahi A., Zali A., Photodegradation of HMX and RDX in the Presence of Nanocatalyst of Znc Slfide Doped with Copper, *Iran. J. Chem. Chem. Eng. (IJCCE)*, **28**: 13-19(2009).